

DRAGON summer research report: charge state distributions after radiative capture

Joel Zylberberg

Simon Fraser University

Supervisor: D. Hutcheon

(Dated: August 3, 2006)

Abstract

DRAGON Measurements of the charge-state distribution (CSD) of a 1.068 MeV/u C beam in He, and of the $6^+ : 5^+$ charge-state population ratio in the recoils of the $^{12}\text{C}(\alpha, \gamma)^{16}\text{O}$ reaction are reported. A computer simulation was developed to model the CSD of both beam and recoil particles in inverse kinematics experiments. The code was used to model this reaction, and the results are compared to data from DRAGON and from ERNA. The simulation was in good agreement with the DRAGON data and with recoil data from ERNA. The results suggest that, for this fusion reaction on the $J^\pi = 4^+$ resonance at $E_{beam} = 1.064$ MeV/u, the recoil ions contain only the nucleons and not the electrons of the target He atom.

Contents

I. Introduction	3
A. Astrophysical importance of the $^{12}\text{C}(\alpha,\gamma)^{16}\text{O}$ reaction	3
B. DRAGON apparatus	4
C. Reaction yields and charge state distributions	5
D. Overview of previous work in this area	6
E. Overview of the current work	6
II. Experimental procedure	7
A. Beam charge-state distribution	7
B. Recoil charge-state distribution	8
III. Experimental results and discussion	9
A. Charge-state distribution of C beam in He	9
B. F_6/F_5 ratio in the recoils of $^{12}\text{C}(\alpha,\gamma)^{16}\text{O}$	10
IV. Simulation	11
A. CSDsim code	11
B. Simulation procedure	13
V. Simulation results and discussion	14
A. Charge-changing cross-sections	14
B. Recoil charge-state distributions and charge-probability matrices	15
VI. Conclusions	21
Acknowledgements	22
A. Cartoons describing the different CP matrix behaviors	23
B. Using the CSDsim code	24
References	25

I. INTRODUCTION

A. Astrophysical importance of the $^{12}\text{C}(\alpha,\gamma)^{16}\text{O}$ reaction

According to big-bang cosmology, most of the light elements (up to ^7Li) were created in the first few minutes of the universe [1]. The heavier elements were created later, in stellar processes.

Main-stage stars (like the sun) are formed when clouds of interstellar gas (mostly hydrogen) collapse due to the gravitational interaction. This collapse causes an increase in the internal temperature of the gas, to the point where nuclear fusion reactions can occur. The outward pressure (thermal and radiation) generated by this hydrogen burning balances the (inward) gravitational force, and the star can remain in this state of hydrostatic equilibrium for an extended period of time.

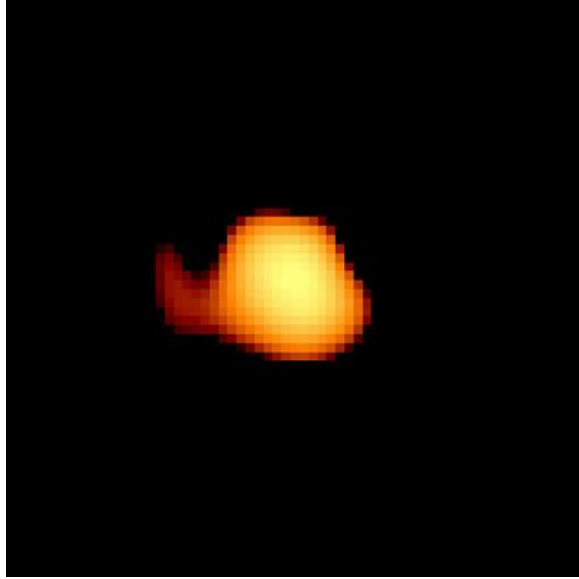


FIG. 1: Image of red giant star Mira taken with the Hubble space telescope [2].

When the supply of hydrogen in the star's core has been depleted, hydrogen burning stops, and the star again begins to collapse. During this collapse, the star heats up, and, if the star is sufficiently large, the outer region (which still contains hydrogen) begins to undergo hydrogen burning. The outward pressure in the outer region of the star then exceeds the inward force of gravity, and the star expands, becoming a red (super)giant (Fig. 1). Meanwhile, the core continues to collapse (and to heat up) until helium burning can

occur [1]. In helium burning, the $3\alpha \rightarrow ^{12}\text{C}$ reaction creates carbon which can subsequently undergo α -capture to form oxygen. It is the relative rates of these two reactions that determines whether oxygen or carbon will be the main product of helium burning in these stars [3]. This provides strong motivation for the measurement of the rates of these reactions, of which one ($^{12}\text{C}(\alpha,\gamma)^{16}\text{O}$) will be discussed in the remainder of this report.

B. DRAGON apparatus

The DRAGON apparatus [4, 5] has been constructed in order to study reactions (such as $^{12}\text{C}(\alpha,\gamma)^{16}\text{O}$) which are of astrophysical interest. In DRAGON experiments, stable or radioactive beams from the TRIUMF-ISAC facility are directed through a windowless gas target consisting of either He or H₂ gas. Through a series of differential pumping tubes, low (10^{-6} Torr) pressures can be maintained in the beamline, while the target is operated at pressures as high as 6 Torr [6].

The beam and recoil particles emerge from the target, and are later separated using magnetic and electric dipoles. The gas target is surrounded by bismuth germanate scintillator detectors (BGO array) which detect the characteristic γ -rays emitted during the radiative capture process. Coincidence is required between the BGO detector and the end detector, which reduces background from beam particles which make it through the separator.

The electromagnetic separator consists of 2 magnetic dipoles (MD) and 2 electric dipoles (ED) in the MD-ED-MD-ED configuration (see Fig. 2). In the MD's, a force $F_{mag} = qvB$ is exerted on the ions, which thereby curve with a radius given by:

$$r = \frac{mv}{qB} \quad (1)$$

Consequently, the MD's separate particles based on their momentum and charge. A slit downstream from the first MD can be adjusted to allow only the desired particles to pass. By similar logic, the ED's steer the particles with a radius

$$r = \frac{mv^2}{qE} \quad (2)$$

The ED, then, separates the particles based on their energy and their charge. A second set of slits downstream from the first ED can, as above, be adjusted to allow only the desired particles to pass. With the use of these and the second MD-ED combination, the

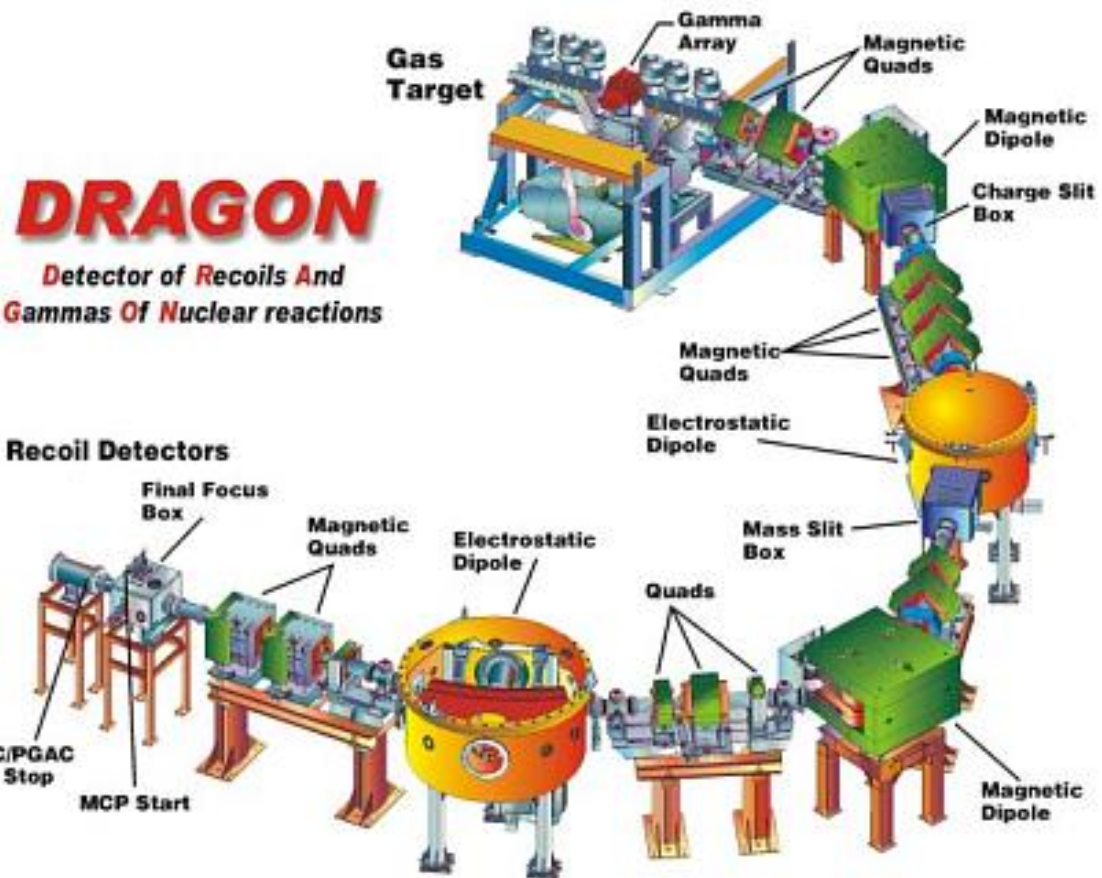


FIG. 2: Schematic overview of the DRAGON apparatus

beam particles can be removed (leaving only the recoils and a small number of “leaky” beam particles) with very high efficiency.

This system can only select one charge state of the beam(recoil) particles for any given separator setting. These ions are detected in the end detector, a double-sided silicon strip detector (DSSSD) which is downstream of the second ED.

C. Reaction yields and charge state distributions

In the laboratory, we measure the rates of reactions of interest by sending a known number of beam particles through the target, and measuring the number of recoils (fusion products) created. For the $^{12}\text{C}(\alpha, \gamma)^{16}\text{O}$ reaction being discussed here, the beam particle is ^{12}C , and the target consists of ^4He gas. Since only particles in one charge state are detected, and the detector efficiency is $\leq 100\%$, the yield per beam particle is calculated as [7]:

$$Yield = \frac{recoils\ detected}{(beam\ particles) \cdot (charge\ state\ fraction) \cdot (detector\ efficiency)}. \quad (3)$$

Thus, in order to determine the reaction yield (and, by corollary, the reaction rate), we must accurately know the fraction F_q of recoils in the charge state selected (where F_q represents the fraction of particles in charge state q).

The charge-state distribution (CSD) of a collection of ions travelling through gas changes as those ions undergo collisions within the gas in which they lose(gain) electrons. For an extended gas target this poses a challenge since the CSD of the recoils will depend on where in the target they were created: those created toward the upstream end pass through the most gas, so they are the most likely to reach an equilibrium CSD [8]. This complication is compounded by the fact that the number of recoils produced per unit distance changes as the beam particles move through the target (as their energy changes due to collisions in the gas, so does the fusion cross-section). This provides the motivation for this work.

D. Overview of previous work in this area

Previous studies at DRAGON [6, 9], ERNA [8] (which is a German electromagnetic recoil spectrometer analogous to DRAGON), and elsewhere [10, 11] have measured the CSD of various beams passing through different gas targets. Of these studies, only one [8] has measured the CSD of the recoils. The Schürmann *et. al.* work [8] investigated the CSD of recoils from the $^{12}\text{C}(\alpha,\gamma)^{16}\text{O}$ reaction. Along with their measurements, Schürmann *et. al.* also tried to predict the CSD of the recoils produced in the He target. Their model assumed that, in the fusion reaction, the charge on the recoil ion was the same as the charge on the beam ion (i.e.: the recoil contains both the electrons and the nucleons of the target particle). This model was in stark disagreement with their data, suggesting that the above assumption may be faulty.

E. Overview of the current work

In this work, measurements of the CSD of the beam and previous DRAGON measurements of the F_6/F_5 ratio in the recoils of the $^{12}\text{C}(\alpha,\gamma)^{16}\text{O}$ reaction on the $J^\pi = 4^+$ resonance at $E_{beam}=1.064$ MeV/u ($E_{c.m.}=3.19$ MeV) are presented along with a computer simulation

(CSDsim) that models the changing CSD of beam and recoil particles as they move through the target. The simulation is then applied to this reaction, and the results are compared to experimental data from DRAGON and ERNA [8] in order to determine how the ion charge changes during the fusion reaction.

II. EXPERIMENTAL PROCEDURE

A. Beam charge-state distribution

Charge-state distributions of carbon ions were measured after a 1.068 MeV/u beam of ^{12}C in the 3^+ charge-state passed through different thicknesses of He gas. The He gas was contained in the windowless gas target system of DRAGON. As described in [4, 5, 12], it consists of a central gas cell having small entrance and exit apertures and a series of differential pumping stages. For hydrogen gas and apertures of 6 and 8 mm, the effective length of the target has been determined to be 123 ± 4 mm [12]. The measurements described here were made with apertures of 4 and 10 mm diameter, which had a combined cross-sectional area 16% larger than that for the 6/8 mm case. A model for gas flow in the system indicated an increase in effective length by about 2 mm should be expected from the increased aperture area, but a decrease by a similar amount when changing from H_2 to He gas. We have assumed the effective length for the He measurements to be 123 mm with an uncertainty of 6 mm. The target temperature was 300 K, with variation of less than 1%, leading to a calculated 3.96×10^{17} atoms/cm² target thickness for a central cell pressure of 1 Torr.

Beam currents were measured in biased faraday cups (FC) at three locations (Fig. 3): (1) FC4 at a beam focus 3.5 m upstream of the gas target, (2) FC1 downstream of the gas target and in front of the first magnetic dipole of the DRAGON separator and (3) FCCH after slits at a focus immediately after the first magnetic dipole. Accordingly, FC4 measured the current of incident 3^+ beam, FC1 measured the beam transmitted through the gas cell summed over all charge-states and FCCH measured the transmitted beam current for one selected charge-state. The charge state fractions could then be calculated as

$$F_q = \frac{I_{FCCH}/q}{I_{FC4}/q_{in}},$$

where I_{FCCH} and I_{FC4} represent the currents at FCCH and FC4, respectively, and q_{in} represents the incident charge state.

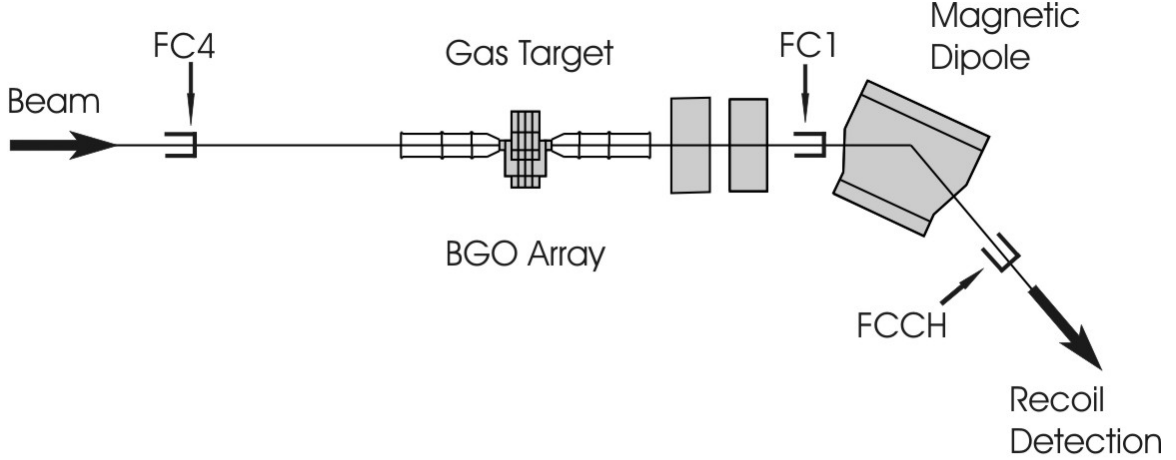


FIG. 3: Diagram of the relevant components of the DRAGON apparatus for the beam CSD measurements. FC denotes a faraday cup.

Beam currents were measured for central cell pressures of 0.25, 0.50, 1.0 and 3.96 Torr. At the two middle pressures, FCCH currents were measured for selected charge-states 4^+ , 5^+ , and 6^+ , while at the other two pressures only charge-states 5^+ and 6^+ were observed. By comparison of the currents in FC4, FC1, and FCCH, it was possible to deduce the beam transmission (80-85%), fractions for the measured charge-states, and at the highest pressure to deduce F_4 . F_3 could not be measured directly because the magnetic dipole did not have enough bending power for C ions of 1.068 MeV/u in that charge-state.

B. Recoil charge-state distribution

These measurements were performed prior to the work term which is the topic of this report. The method used to perform these measurements is, however, included in this report for the sake of completeness.

The full DRAGON system of gas target, gamma-detection (bismuth germanate scintillators: BGO) array, mass separator and recoil particle detector was used to detect the gamma rays and ^{16}O recoil ions which result from radiative alpha capture by ^{12}C into the $J^\pi = 4^+$ resonance at $E_{cm} = 3.19$ MeV. The BGO array had a hardware threshold set to trigger

upon detection of either or both members of the 3.5 and 6.9 MeV cascade, giving a trigger efficiency of approximately 70%. Energy of the recoil ions was registered in a double-sided silicon-strip detector (DSSSD) at the end of the separator. The standard (for proton capture experiments) downstream pumping tubes of the gas target were replaced by a set having a nominal acceptance half-angle of 25 mrad. Yields were measured as the number of BGO–DSSSD coincidences, normalized to counts in a Si-surface barrier detector which counted alpha particles from elastic scattering of the beam in the He gas target. The coincidence requirement ensured a background-free signal, even at the lowest gas pressures.

The beam energy was adjusted to give maximum yield of recoil ions at a target pressure of 3.96 Torr. The relative yields of 5^+ and 6^+ recoil ions were measured at this pressure and at 0.25, 0.50 and 1.0 Torr without any further adjustment of beam energy. The 4^+ recoil yields could not be measured because the DSSSD would have been swamped by a low-energy tail of the ^{12}C beam in the 3^+ charge-state, which has the same mass/charge ratio and therefore could not be eliminated by the separator.

III. EXPERIMENTAL RESULTS AND DISCUSSION

A. Charge-state distribution of C beam in He

Table I shows our results for the CSD of a C^{3+} beam in a He target at 12.82 MeV, while Table II shows previously unpublished DRAGON results [9] for the CSD of a C^{3+} beam in a He target at 12.0 MeV. The uncertainties in our data come from a 5% uncertainty in the transmission value, and a 10 epA uncertainty on each FC measurement, which were added in quadrature. It should be noted that, in our data, there is a 5% scale uncertainty in target thickness associated with the uncertainty in effective target length.

Our value for F_6 after a 3.96 Torr He target is in excellent agreement with a previous polynomial fit for $F_6(P, E)$ [9]. This fit is valid only for DRAGON target pressures above 3 Torr, so it cannot be used to verify the lower-pressure data points. Nevertheless, this agreement confirms the accuracy of our measurement.

The main differences between the data sets in Tables I and II are that they were measured at (slightly) different energies, and that the analysis used to extract the data in Table II assumed that the population of the 3^+ charge-state was zero, while our analysis made no

TABLE I: Measured charge-state distributions of 12.82 MeV C³⁺ beam in He target.

Pressure (Torr)	F_4	F_5	F_6
3.96	0.17±0.03	0.54±0.03	0.292±0.015
1.0	0.41±0.02	0.50±0.02	0.084±0.004
0.5	0.57±0.03	0.274±0.014	0.021±0.0011
0.25	not measured	0.10±0.005	0.005±0.0003

such assumption. Despite these discrepancies, there is still useful information in Table II: the equilibrium CSD is reached with a DRAGON target pressure of roughly 3 Torr. Since these data points were collected at an energy similar to the 12.82 MeV beam energy used in the current study, it suggests that, at the present energy as well, equilibrium is likely reached near that 3 Torr pressure.

 TABLE II: Measured charge-state distributions of 12.0 MeV C³⁺ beam in He target; previously unpublished data from Ref. [9].

Pressure (Torr)	F_4	F_5	F_6
5.35	0.140	0.583	0.277
3.99	0.156	0.588	0.257
3.09	0.180	0.589	0.231
2.08	0.197	0.613	0.191
1.26	0.286	0.517	0.197
0.72	0.557	0.407	0.037

B. F_6/F_5 ratio in the recoils of $^{12}\text{C}(\alpha,\gamma)^{16}\text{O}$

The measured F_6/F_5 ratios in the recoils at several different pressures are shown in Table III. The uncertainties in this data come from the relative statistical uncertainties in

the number of counts for the 5^+ and 6^+ states, which were added in quadrature.

The data set shows a non-linear variation in the F_6/F_5 ratio over the pressure range studied. This variation provides strong motivation for the development of the CSDsim code, since an accurate knowledge of the recoil CSD is needed in order to properly analyze experimental data. The mechanism behind this variation is discussed below.

TABLE III: Measured F_6/F_5 ratio in the recoils of $^{12}\text{C}(\alpha,\gamma)^{16}\text{O}$ on the $J^\pi = 4^+$ resonance.

Pressure (Torr)	F_6/F_5
3.96	0.68 ± 0.04
1.0	0.96 ± 0.08
0.5	0.92 ± 0.10
0.25	0.82 ± 0.10

There is no other data with which to compare these results, as Schürmann *et al.* did not report F_5 in the recoils from their experiment.

IV. SIMULATION

A. CSDsim code

The CSDsim code was written in C programming language, and is essentially a numerical integrator (with a few extra features: to be discussed in this section) that solves the set of coupled differential equations (4) which describes the changing CSD of a group of particles traveling through matter [6]. Since the energy losses are quite low in the inverse-kinematics experiments that CSDsim models, the charge-changing cross-sections are assumed to be constant throughout the simulation.

$$\frac{dF_q}{dx} = \sum_{q', q' \neq q} (F_{q'} \sigma_{q', q} - F_q \sigma_{q, q'}) \quad (4)$$

Equation (4) is bound by condition (5) [6].

$$\sum_q F_q = 1 \quad (5)$$

For each slice of the target (a user-defined variable: 10^{13} atoms/cm² was used for the simulations discussed here), the program recalculates the CSD of the beam and (existing) recoils using Eq. (4). It then calculates the energy of the beam, assuming linear energy loss (which is suitable for the relatively small energy losses being discussed here), using dE/dx values from the SRIM2003 Tables [13]. CSDsim then calculates an updated fusion cross-section from a Breit-Wigner-type equation (6), which allows it to model the changing number of recoils produced in each slice of the target.

$$\sigma_{fusion} = \sigma_{max} \left(1 + \left(\frac{E_{beam} - E_{resonance}}{\frac{\Gamma_{total}}{2}} \right)^2 \right)^{-1} \quad (6)$$

The CSD of the recoils being created is then calculated by multiplying the beam CSD matrix by a matrix which describes the probability of creating a recoil of a given charge for each possible beam charge-state (charge-probability or CP matrix). As an example, the general CP matrix for the ${}^4\text{He}({}^3\text{H},\gamma){}^7\text{Li}$ reaction with a ${}^4\text{He}$ beam is

$$CP \text{ matrix} = \begin{pmatrix} P_{0,0}P_{1,0}P_{2,0} \\ P_{0,1}P_{1,1}P_{2,1} \\ P_{0,2}P_{1,2}P_{2,2} \\ P_{0,3}P_{1,3}P_{2,3} \end{pmatrix},$$

where $P_{a,b}$ represents the probability of creating a recoil of charge b from a beam ion of charge a .

The resultant “new” recoil CSD is then multiplied by the number of recoils to be added in the slice ($dx \cdot \sigma_{fusion}$), and added to the existing recoil CSD matrix (which has been multiplied by the number of existing recoils). Finally, CSDsim normalizes the recoil CSD matrix so that Eq. (5) is obeyed.

For each slice of the target, CSDsim also calculates the energy of the recoils being produced (which is assumed to be constant over all recoils). By assuming that the momentum of the recoils is roughly the same as that of the beam particles, the energy of the recoils is calculated to be

$$E_{recoil} = E_{beam} \frac{m_{beam}}{m_{recoil}}, \quad (7)$$

where m_{beam} and m_{recoil} are the masses of the beam and recoil particles, respectively.

CSDsim outputs the beam and recoil CSD, the average energy of the beam and recoil particles, and the total number of recoils created in the last cycle after a user-defined number of cycles (100 for the simulations discussed here). The resultant data files can be used in acceptance simulations, where the geometric location of recoil production is important, and in analyzing data, where the CSD of the beam and recoils are important.

Access to and use of the CSDsim code are discussed below, in appendix B.

B. Simulation procedure

To start, we fit a set of charge-changing cross-sections (CCCS's) to experimental data for a C beam in He at 12.82 MeV (from this work) and for an O beam in He at 9.6 MeV [8] [which is the energy of the oxygen recoils, according to Eq. (7)]. In each case, this was done by first finding a nominal CCCS set, and then using a least-squares algorithm to find the “best” CCCS's and the uncertainties therein.

The generated CCCS sets account for single-electron losses and gains only, as the CCCS's for multiple-electron processes in He gas are known to be quite small [10].

The nominal CCCS sets were found by first setting the ratios of the CCCS's to be such that the correct equilibrium CSD was reached, i.e. Eq. (8), and then scaling the individual $\sigma_{q,q'}$, $\sigma_{q',q}$ pairs together (multiplying them both by the same value) until the charge-state populations changed at a rate that agreed roughly with the experimental data.

$$\frac{\sigma_{q,q'}}{\sigma_{q',q}} = \frac{F_{q'}}{F_q} \quad (8)$$

Once these nominal CCCS's were found, we iteratively recalculated the resultant CSD, each time perturbing one of the CCCS's by $\pm 10\%$ from the nominal value. The χ^2 value (9) for each of these CSD's (as compared with the experimental data in which the uncertainties were normalized so that χ^2 per degree of freedom was 1) was then calculated. Next, we fit a parabola to the χ^2 vs $\sigma_{q,q'}$ distribution, which allowed us to determine the best CCCS and the uncertainty on the cross-section (the deviation from the “best” CCCS for which the χ^2 value increased by 1). In each case, this process was repeated twice in order to ensure the reliability of the CCCS's.

$$\chi^2 = \sum \left(\frac{F_{observed} - F_{calculated}}{\Delta F_{observed}} \right)^2 \quad (9)$$

In cases where the equilibrium ratio between states q and $q + 1$ was known, only the electron loss CCCS (i.e.: $\sigma_{q,q+1}$) was found in the above manner, and the corresponding electron capture CCCS ($\sigma_{q+1,q}$) was determined by Eq. (8). In these instances, the estimated error on the electron capture CCCS was the result of adding, in quadrature, the error on the electron loss CCCS, and the uncertainty in the equilibrium charge-state population ratio.

Once we had determined the CCCS's, we investigated how changing the CP matrix (which describes the electron loss/capture behavior during fusion) affected the behavior of the model by comparing CSDsim predictions using different CP matrices to data for F_6 [8], and the F_6/F_5 ratio in the recoils of $^{12}\text{C}(\alpha, \gamma)^{16}\text{O}$. The CP matrices studied reflected several different physically plausible behaviors (these are shown in cartoons in appendix A):

1. the recoil Picks Up both electrons (PU2e) of the target particle, thus $q_{recoil} = q_{beam}$ (this is the assumption made in Ref. [8]);
2. the recoil Picks Up none of the electrons (PU0e) from the target, thus $q_{recoil} = q_{beam} + 2$;
3. the ratios between the Charge-State Probabilities are the same as the ratios between the Equilibrium Fractions (CSPEF) of the recoils;
4. the Charge-State Probabilities are such that they Maximize production in the 5^+ State (CSPM5S) (which has the largest population at equilibrium [8]);
5. the charge-state probabilities are a mixture PU2e and PU0e behavior.

V. SIMULATION RESULTS AND DISCUSSION

A. Charge-changing cross-sections

The data for CSD as a function of target thickness for a C^{3+} beam at 12.82 MeV (from this work) and an O^{3+} beam at 9.6 MeV (from ref [8]) in a He target are shown in Figs. 4 and 5, respectively. Also shown in these figures are the CSDsim fits to the data. In both cases, the agreement between the CSDsim fit and the experimental data confirms the validity of our model.

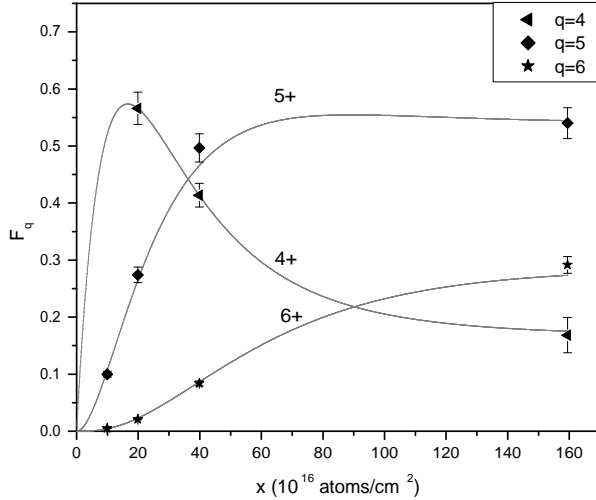


FIG. 4: Charge-state fractions as a function of target thickness for a 12.82 MeV C^{3+} beam in He. The solid lines are CSDsim predictions using the fitted cross-sections (see text).

Our CCCS's are listed in Tables IV and V along with CCCS's from Ref. [10]. Direct comparison of these CCCS sets is difficult since these CCCS sets are for different energies, and there is strong nonlinearity in the velocity (energy) dependence of the CCCS's [14]. However, a comparison between our CCCS's for a 12.82 MeV C beam in He and those of Dillingham *et al.* (for a 12 MeV E_{beam}) shows that, in all cases, the Dillingham *et al.* CCCS's are roughly 70 – 80% as large as ours, which is reasonably good agreement between these CCCS sets. Comparison between our CCCS's and those of Dillingham *et al.* for a 13.6 MeV E_{beam} are not as good: the Dillingham *et al.* CCCS's range from 30% to 70% of ours.

B. Recoil charge-state distributions and charge-probability matrices

Figure 6 shows the F_6/F_5 ratio in the recoils for simulations with various CP matrices (representing behaviors 1-5, see Simulation Procedure section for details), along with experimental data from this work. The agreement between the simulation and the experiment is quite good for a PU0e CP matrix (see Simulation Procedure section for details), and becomes progressively worse as the CP matrix is modified to include more of the PU2e behavior. Similarly, CP matrices which reflect PU2e, CSPEF, and CSPM5S behavior are all in strong disagreement with the data. This suggests that, in the ${}^{12}\text{C}(\alpha, \gamma){}^{16}\text{O}$ reaction

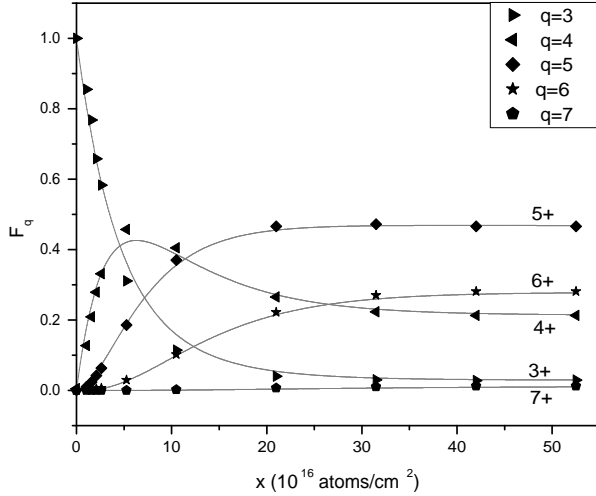


FIG. 5: Charge-state fractions as a function of target thickness for an 9.6 MeV O^{3+} beam in He. The solid lines are CSDsim predictions using the fitted cross-sections (see text). The data shown are results from Ref. [8].

TABLE IV: Charge-changing cross-sections for C in He, in 10^{-18} cm 2 /atom; comparison between those developed in this work and those listed in Ref. [10].

CCCS	Dillingham	This work		Dillingham
		12 MeV	(12.82 MeV)	
$\sigma_{6,5}$	1.77 ± 0.17	2.2 ± 0.2	0.813 ± 0.046	
$\sigma_{5,6}$	0.723 ± 0.048	1.14 ± 0.06	0.823 ± 0.044	
$\sigma_{5,4}$	0.868 ± 0.037	1.1 ± 0.2	0.361 ± 0.022	
$\sigma_{4,5}$	none listed	3.5 ± 0.1	none listed	
$\sigma_{4,3}$	none listed	0.4 ± 0.5	none listed	
$\sigma_{3,4}$	none listed	10.3 ± 0.4	none listed	

(at 1.06 MeV/u in the lab frame), immediately after fusion, the recoils do not contain the electrons of the target particle.

Similarly, Fig. 7 shows both data (from Ref. [8]) and simulation results (CSDsim and the simulation used in Ref. [8]) for F_6 in the recoils. The results for a simulation with PU2e behavior (the assumption made by Schürmann *et al.*) agree qualitatively with the prediction

TABLE V: Charge-changing cross-sections for O in He, in $10^{-18} \text{ cm}^2/\text{atom}$; comparison between those developed in this work and those listed in Ref. [10].

	CCCS Dillingham	This work	Dillingham
	9 MeV	(9.6 MeV)	16 MeV
$\sigma_{7,6}$	24.0±1.2	6±3	2.48±0.07
$\sigma_{6,7}$	none listed	0.25±0.12	none listed
$\sigma_{6,5}$	none listed	13±3	none listed
$\sigma_{5,6}$	none listed	7.8±1.4	none listed
$\sigma_{5,4}$	none listed	7.3±0.8	none listed
$\sigma_{4,5}$	none listed	16±1	none listed
$\sigma_{4,3}$	none listed	2.9±0.3	none listed
$\sigma_{3,4}$	none listed	20.9±0.5	none listed

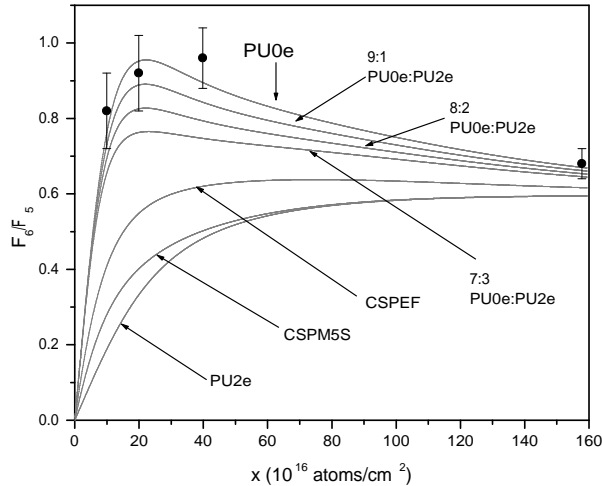


FIG. 6: F_6/F_5 ratio in the recoils of $^{12}\text{C}(\alpha,\gamma)^{16}\text{O}$ as a function of target thickness. The solid lines are CSDsim predictions using different recoil charge-probability matrices (see text).

made by Schürmann *et al.*, and both of these predictions fail to match the data. However, as in the above case of comparison with our results, the simulation with PU0e behavior is in much better agreement with the data. Unlike the above case, however, the CSDsim predictions with PU0e behavior still do not provide good agreement with this data set.

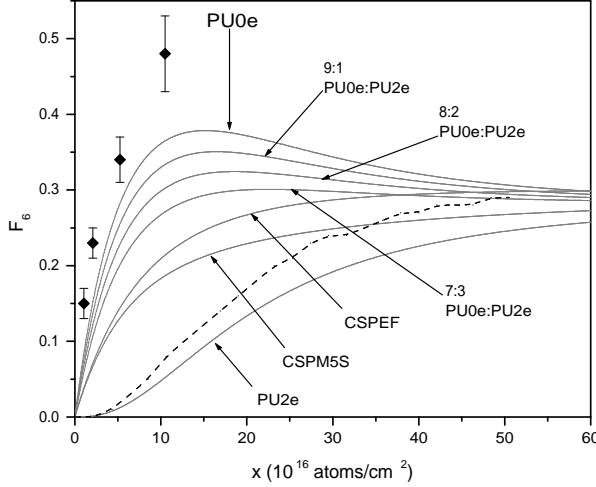


FIG. 7: F_6 in the recoils of $^{12}\text{C}(\alpha, \gamma)^{16}\text{O}$ as a function of target thickness. The solid lines are CSDsim predictions using different recoil charge-probability matrices (see text). The data shown are results from Ref. [8]. The dashed line is the result of the simulation used in Ref. [8].

In an attempt to improve the agreement between the CSDsim predictions and the Schürmann *et al.* data, simulations were performed in which the PU0e behavior was modified so that Li-like (C^{3+}) beam ions form a mixture of Li-like (O^{5+}) and He-like (O^{6+}) species in the fusion reaction (in addition to not gaining any electrons (PU0e behavior) during the fusion reaction, we allowed for the possibility that some may be lost). As an example, the CP matrix for PU0e behavior, modified so that Li-like beam ions form 90% Li-like and 10% He-like recoils, is

$$M_{90:10} = \begin{pmatrix} 0 & 0 & 0 & 0 & 0 & 0 & 0 \\ 0 & 0 & 0 & 0 & 0 & 0 & 0 \\ 1 & 0 & 0 & 0 & 0 & 0 & 0 \\ 0 & 1 & 0 & 0 & 0 & 0 & 0 \\ 0 & 0 & 1 & 0 & 0 & 0 & 0 \\ 0 & 0 & 0 & 0.9 & 0 & 0 & 0 \\ 0 & 0 & 0 & 0.1 & 1 & 0 & 0 \\ 0 & 0 & 0 & 0 & 0 & 1 & 0 \\ 0 & 0 & 0 & 0 & 0 & 0 & 1 \end{pmatrix}.$$

The results of these simulations are shown alongside data from this work and from Ref. [8]

in Figs. 8 and 9, respectively. All of the curves shown (which represent different Li-like:He-like O recoil ratios from Li-like C ions) are in good agreement with our data. However, for comparison with the Schürmann *et al.* data, this is not the case: the 90:10 Li-like:He-like recoil model is clearly the best.

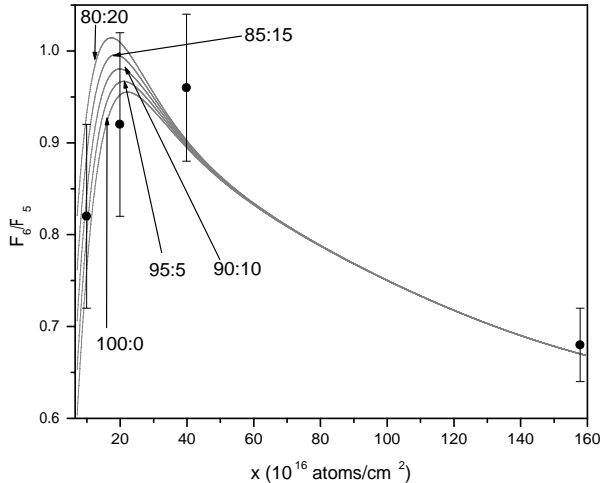


FIG. 8: F_6/F_5 ratio in the recoils of $^{12}\text{C}(\alpha,\gamma)^{16}\text{O}$ as a function of target thickness, where PU0e behavior with additional electron loss was modeled. The solid lines are CSDsim predictions which are labeled according to the ratio of Li-like:He-like recoils being created from Li-like beam ions.

The broad peak in the F_6/F_5 ratio in the recoils can be understood by observing how the CSD of the carbon beam changes in the He target. In Fig. 4, it can be seen that there is a peak in the C^{4+} fraction at a depth of roughly 1.7×10^{17} atoms/cm 2 . This corresponds closely to the approximately 2.2×10^{17} atoms/cm 2 depth at which the F_6/F_5 ratio is seen to peak. We have already seen that, at this depth, the majority of the recoils have a charge 2 greater than that on the beam ion. Thus, we can infer that the peak in the recoil F_6/F_5 ratio comes from the increased C^{4+} charge-state fraction at that depth.

It should be noted that CSDsim shows low sensitivity to certain CP matrix elements. In particular $P_{6,8}$ and $P_{6,7}$ can be interchanged in the above matrix without noticeably changing the predicted recoil CSD. Similarly, a reduction in $P_{5,7}$ (with a subsequent increase in $P_{5,8}$) causes no noticeable change in the predicted CSD over the whole (0 – 1) range of possible values. This is because $\sigma_{8,7} \gg \sigma_{7,8}$ (at 9 MeV [10]), thus any recoils produced in the 8^+ state quickly change to the 7^+ state. Furthermore, reductions in $P_{5,7}$ (with subsequent increases

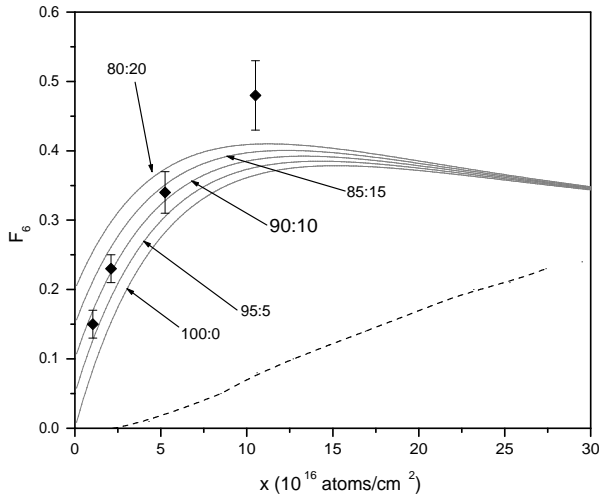


FIG. 9: F_6 in the recoils of $^{12}\text{C}(\alpha,\gamma)^{16}\text{O}$ as a function of target thickness, where PU0e behavior with additional electron loss was modeled. The solid lines are CSDsim predictions which are labeled according to the ratio of Li-like:He-like recoils being created from Li-like beam ions. The data shown are results from Ref. [8]. The dashed line is the result of the simulation used in Ref. [8].

in $P_{5,6}$) do cause noticeable changes in the F_6 and F_6/F_5 predictions of CSDsim, but over the range of possible values, the predictions all agree equally well with the F_6/F_5 data (from this work) and the F_6 data from ERNA [8].

Despite the limitations of our model, the results clearly show that electron capture and loss probabilities at the time of a nuclear capture reaction are different from the average probabilities experienced by ions which pass completely through a gas target. Capture reactions involve special conditions such as small (on the atomic scale) impact parameters and violent deceleration of the incident beam nucleus. However, it is not clear whether these features are the explanation for the difference in probabilities. Another open question is whether the behavior is specific to this beam energy (an “accident” due to atomic shell effects, say) or is a general feature of capture reactions.

In the absence of a proven, universal model for atomic charge changes during a capture reaction, special measures may be needed for certain radiative capture experiments with a gas target and recoil separator. Such cases include narrow resonances near the downstream end of the target or reactions (broad resonances or direct capture) which occur throughout the entire length of the target. One approach, adopted at ERNA, is to add a post-stripper

gas cell to bring all recoil ions to a known equilibrium charge-state distribution [8]. Another possibility is to use a thin stripper foil after the gas target, as successfully demonstrated in the $^{40}\text{Ca}(\alpha, \gamma)^{44}\text{Ti}$ reaction at DRAGON [15].

In the limiting case of a very thick target, however, these precautions are unnecessary since the recoil CSD is the same as that of an oxygen beam passing through a He target; the recoil CSD is independent of the electron loss/capture behavior during fusion. For a reaction with a constant fusion cross-section, at a DRAGON target pressure of 4(8) Torr, making this thick-target assumption results in an overestimation of F_5 by 12(5)%, and an underestimation of F_6 by 0.4(-0.2)% (when compared to the PU0e prediction). Similarly, at 4(8) Torr, the differences between the PU2e and PU0e predictions for F_5 and F_6 are 13(6)%, and 1(0.5)%, respectively. Thus, another useful approach is to use a target of sufficient thickness that the uncertainty in the recoil CSD is minimized.

If none of the above methods can be used, then one can partition the experimental time, selecting recoils in the 2 or 3 most probable charge-states for separate yield measurements.

VI. CONCLUSIONS

We have discussed measurements of the CSD of a C^{3+} beam in a He target, as a function of target thickness, as well as the ratio of F_6/F_5 in the recoils of the $^{12}\text{C}(\alpha, \gamma)^{16}\text{O}$ reaction on the $J^\pi = 4^+$ resonance.

The CSDsim code has been written and used to model this reaction in order to ascertain the change in the charge on a beam particle at the moment of the fusion reaction. The CSDsim code can provide good agreement with our results and those from Ref. [8]. The best agreement with experiment comes when the model assumes that, at the moment of fusion, none of the electrons from the target He atom are captured. Furthermore, it appears that some of the recoils contain even fewer electrons than did the beam particles, indicating that some additional electrons may be lost during the fusion process. Our results were sensitive to the CSD of recoils produced from α capture by C^{3+} and C^{4+} beam ions. More data is needed in order to develop a thorough understanding of the CSD following α capture by C^{5+} or C^{6+} ions.

These results imply that it is, in some cases, necessary to measure the recoil CSD for inverse-kinematics experiments, because simplifying assumptions (like $q_{beam} = q_{recoil}$) are

not necessarily accurate.

This knowledge, along with the capabilities of the CSDsim code, are useful to those studying nuclear fusion reactions in inverse kinematics, like at DRAGON and ERNA.

This is the first time that the recoil charge-state distribution has been successfully modeled. As such, an abbreviated version of this report has been submitted for publication in Nuclear Instruments and Methods in Physics Research section B.

Acknowledgements

The author would like to thank Dr. D. Hutcheon and the rest of the DRAGON group for helpful discussion and support during this work. The help of D. Hutcheon in writing the experimental procedure section of this report is also acknowledged. Financial support from the Natural Sciences and Engineering Research Council of Canada and TRIUMF are gratefully acknowledged. The author would further like to thank Dr. D. Schürmann for providing us with numerical values for the data from ERNA.

APPENDIX A: CARTOONS DESCRIBING THE DIFFERENT CP MATRIX BEHAVIORS

These figures are included because it is expected that some readers will find the abstract descriptions of the charge-changing behaviors during fusion difficult to follow.

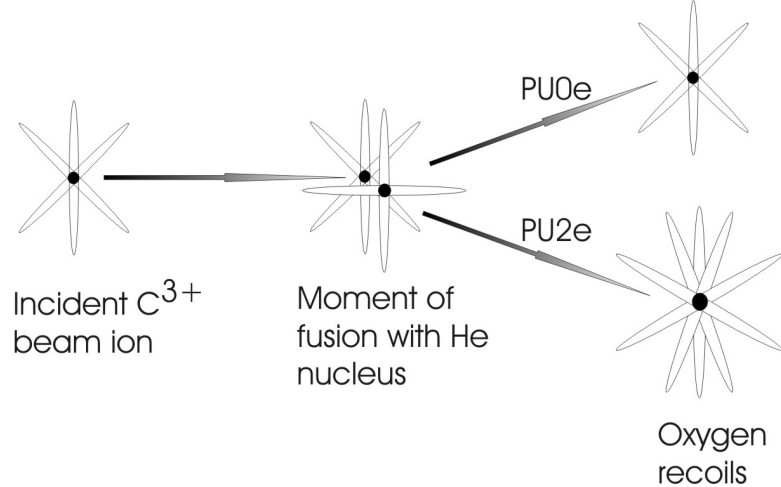


FIG. 10: Cartoon describing the PU0e and PU2e behaviors during fusion. In these scenarios, the recoil contains neither (PU0e) or both (PU2e) of the electrons of the target atom, immediately after fusion.

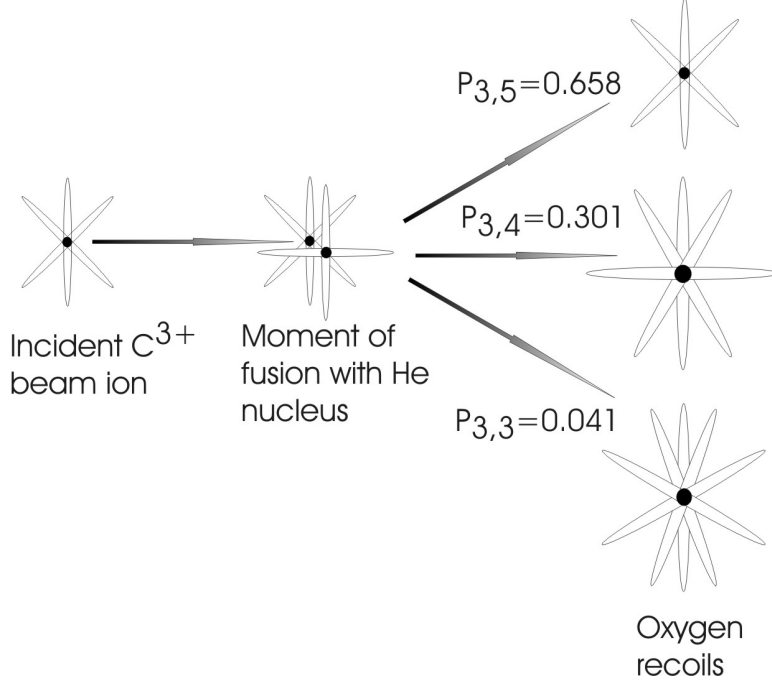


FIG. 11: Cartoon describing the CSPEF behavior during fusion. In this scenario, the probability of capturing 0, 1, or 2 electrons during fusion is governed by the relative populations of those charge-states in an equilibrium O beam (in He gas).

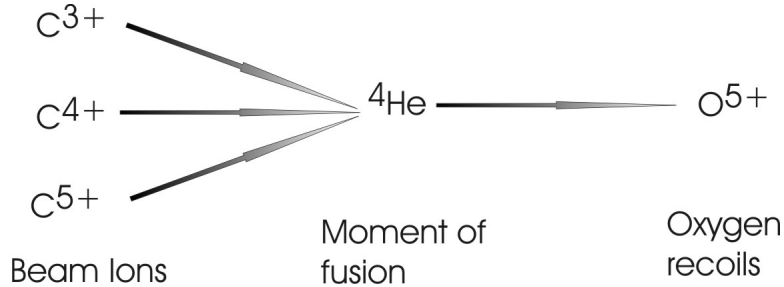


FIG. 12: Cartoon describing the CSPM5S behavior during fusion. In this scenario, every beam charge-state that can produce recoils in the 5^+ charge-state does so.

APPENDIX B: USING THE CSDSIM CODE

CSDsim was written in a very general way, and will work for any inverse kinematics experiment. The items which need to be updated for this to work have all been defined in the preprocessor directives of the code (this includes recoil and projectile atomic numbers, etc.). CSDsim was compiled with the CC compiler. Other C compilers may work fine, but troubles may be encountered.

The CCCS's for the beam and recoil particles, and the CP matrix are input as data files, with no headers, in which the entries are tab delimited. The output files contain no headers, and are space delimited. The first column of the file is the depth (in units of 10^{16} atoms/cm 2), and subsequent columns are the F_q for q from 0 to Z (where Z is the atomic number of the beam or recoil particle, depending on the file selected).

CSDsim and the associated cross-section and CP matrix files are located in the home/-dragon/JoelZ/CSDsim folder of the ast05 computer at TRIUMF. They can also be found in the joelz/CSDsim_stuff folder of the DRAGON account on IBM00. Finally, they can be downloaded from <http://www.sfu.ca/~jzylberb/CSDsim>.

- [1] C. Rolfs and W.Rodney, Cauldrons in the Cosmos (University of Chicago Press, 1988).
- [2] Image from the Hubble space telescope website
http://hubblesite.org/gallery/album/entire_collection/pr1997026d/, accessed August 2006.
- [3] L.R. Buchmann, C.A. Barnes, Nuclear reactions in stellar helium burning and later hydrostatic burning stages, Nucl. Phys. A, in press.
- [4] D.A. Hutcheon, S. Bishop, L. Buchmann, M.L.Chatterjee, A.A. Chen, J.M. D'Auria, S. Engel, D. Gigliotti, U. Greife, D. Hunter, A. Hussein, C.C. Jewett, N. Khan, M. Lamey, A.M. Laird, W. Liu, A. Olin, D. Ottewell, J.G. Rogers, G. Roy, H. Sprenger, C. Wrede, Nucl. Instr. and Meth. A 498 (2003) 190.
- [5] S. Engel, D. Hutcheon, S. Bishop, L. Buchmann, J. Caggiano, M.L. Chatterjee, A.A. Chen, J. D'Auria, D. Gigliotti, U. Greife, D. Hunter, A. Hussein., C.C. Jewett, A.M. Laird, M. Lamey, W. Liu, A. Olin, D. Ottewell, J. Pearson, C. Ruiz, G. Ruprecht, M. Trinczek, C. Vockenhuber, C. Wrede, Nucl. Instr. and Meth. A 553 (2005) 491.
- [6] W. Liu, G. Imbriani, L. Buchmann, A.A. Chen, J.M. D'Auria, A. D'Onofrio, S. Engel, L. Gialanella, U. Greife, D. Hunter, A. Hussein, D.A. Hutcheon, A. Olin, D. Ottewell, D. Rogalla, J. Rogers, M. Romano, G. Roy, F. Terrasi, Nucl. Instr. and Meth. A 496 (2003) 198.
- [7] H. Crawford, Beam normalization for the $^{26}\text{Al}(\text{p},\gamma)^{27}\text{Si}$ reaction; Calibration of the DSSSD, Practicum Report, http://dragon.triumf.ca/docs/BeamNormalization_HC.pdf, 2005.
- [8] D. Schürmann, F. Strieder, A. Di Leva, L. Gialanella, N. De Cesare, A. D'Onofrio, G. Imbriani,

- J. Klug, C. Lubritto, A. Ordine, V. Roca, H. Rocken, C. Rolfs, D. Rogalla, M. Romano, F. Schumann, F. Terrasi, H.P. Trautvetter, Nucl. Instr. and Meth. A 531 (2004) 428.
- [9] W.R. Hannes, Beam Current and Target Density Normalization in E952 $^{12}C(\alpha, \gamma)^{16}O$ at DRAGON, Practicum Report, <http://dragon.triumf.ca/docs/Wolf-report.pdf>, 2005.
- [10] T.R. Dillingham, J.R. Macdonald and P. Richard, Phys. Rev. A. 24 (1981) 1237.
- [11] J.R. Macdonald and F.W. Martin, Phys. Rev. A. 4 (1971) 1965.
- [12] U. Greife, S. Bishop, L. Buchman, M.L. Chatterjee, A.A. Chen, J.M. D'Auria, S. Engel, D. Gigliotti, D. Hunter, D.A. Hutcheon, A. Hussein, C.C. Jewett, A.M. Laird, M. Lamey, W. Liu, A. Olin, D. Ottewell, J. Rogers, C. Wrede, Nucl. Instr. and Meth. B 217 (2004) 1.
- [13] J.F. Ziegler, J.P. Biersack, and U. Littmark, The Stopping and Range of Ions in Matter, <http://www.srim.org>, 2003.
- [14] G. Shiwietz and P.L. Grande, Nucl. Instr. and Meth. B 175 (2001) 125.
- [15] C. Vockenhuber, C.O. Ouellet, L. Buchmann, J. Caggiano, A.A. Chen, J.M. D'Auria, D. Frekers, A. Hussein, D.A. Hutcheon, W. Kutschera, K. Jayamanna, D. Ottewell, M. Paul, J. Pearson, C. Ruiz, G. Ruprecht, M. Trinczek, A. Wallner, The $^{40}\text{Ca}(\alpha, \gamma)^{44}\text{Ti}$ reaction at DRAGON, Nucl. Instr. and Meth. B, submitted.